An Augmented Reality Haptic Training Simulator for Spinal Needle Procedures

Colin Sutherland, *Student Member, IEEE,* Keyvan Hashtrudi-Zaad, *Senior Member, IEEE,*
Rick Sellens, *Senior Member, IEEE,* Purang Abolmaesumi, *Senior Member, IEEE,*
Parvin Mousavi, *Senior Member, IEEE*

Abstract—This paper presents the prototype for an augmented reality haptic simulation system with potential for spinal needle insertion training. The proposed system is composed of a torso mannequin, a MicronTracker2 optical tracking system, a PHANToM haptic device and a graphical user interface to provide visual feedback. The system allows users to perform simulated needle insertions on a physical mannequin overlaid with an augmented reality cutaway of patient anatomy. A tissue model based on a finite element model provides force during the insertion. The system allows for training without the need for the presence of a trained clinician or access to live patients or cadavers. A pilot user study demonstrates the potential and functionality of the system.

Index Terms—Haptics, Augmented Reality, Medical Simulator.

I. INTRODUCTION

VIRTUAL reality (VR) medical training simulators have become more common in hospitals and teaching centers to train medical students and residents procedures that they will need to perform in the operating room. Simulators allow a user to interact with a virtual scene representing the procedure, normally with a form of force feedback to provide forces that would be present during the procedure. In contrast to conventional training methods for medical procedures (such as those for spinal taps and laparoscopic surgery) that are mostly based on trial and error on phantoms, cadavers and actual patients, simulators provide flexible training opportunities as trainees do not require the direct supervision of trained clinicians or access to cadavers and patients. This has multiple benefits: the strain on the limited and valuable time of trained clinicians is reduced, the risk of complications from inexperienced students performing procedures on patients is decreased , and patients with various body types and conditions can be simulated without the need for a patient or cadaver to be present.

The two main types of training systems in the literature are Virtual Reality (VR) based and mannequin based [1]. Purely haptic based virtual medical training systems are by far the most common form of simulators in the literature

C. Sutherland and K. Hashtrudi-Zaad are with the Department of Electrical and Computer Engineering, Queen's University, Kingston, ON, Canada.

R. Sellens is with the Department of Mechanical Engineering, Queen's University, Kingston, ON, Canada.

P. Abolmaesumi is with the Department of Electrical and Computing Engineering, University of British Columbia, Vancouver, BC, Canada.

P. Mousavi is with the School of Computing, Queen's University, Kingston, ON, Canada e-mail: (pmousavi@cs.queensu.ca).

Manuscript received MONTH DAY, YEAR; revised MONTH DAY, YEAR.

[2], [3], [4]. VR systems can easily create a variety of virtual environments that can be explored by means of virtual tools that are controlled through the interaction between the user interacts and the input (haptic) device. The environment is commonly created from medical imaging volumes such as ultrasound (US), Magnetic Resonance Imaging (MRI) or Computed Tomography (CT). The imaging volumes are used as the basis for different force models that determine the force that the haptic device need to output to the user. Users can also view the patient data being explored on a computer monitor.

Spinal needle insertion simulators have been proposed for core needle biopsy, anesthetic injection or vertebroplasty. Likewise other applications, spinal needle insertion simulators are mostly haptic based [5], [6], [7], [8].

A lumbar puncture training system presented by Farber *et al.* uses a PHANToM Premium 1.5A haptic device with six active degree-of-freedom (DOF) [5]. This allows the system to completely constrain the virtual needle (represented by the haptic device) when it enters tissue. Force feedback during needle insertion is provided by Hooke's law for linear spring models and a proxy-based algorithm. The only form of visual feedback in this system is the 3D CT volume shown on a computer monitor, along with the position of the virtual needle.

US guided needle insertion simulators for biopsy are proposed by Vidal *et al.* [6] and Chan *et al.* [7]. The former uses two PHANToM Omni™ haptic devices to represent an US probe and biopsy needle. A patient CT volume specifies the virtual environment, and force is provided through a proxy-based approach. The latter presents a training system through a game environment where users must seek a target with an US probe and then needle prior to performing an insertion with real patient data. When tracking targets that are simulated by spheres in a homogeneous volume, images are simulated from a slice of the volume, while when performing insertions a 3D US volume is re-sliced. The US image is deformed using a mass-spring model, however this deformation is applied directly to the re-slice of the US volume.

The work presented in [8] is seemingly the most intricate VR simulation system reported in the literature. It introduces a vertebroplasty simulator in the form of a computer game-like environment, and uses various haptic devices to convey the sense of operation. To provide force feedback for needle insertion, a customized Delta™, haptic device with six active DOF and high stiffness is used, along with an Immersion CyberGlove™and CyberGrasp™to provide accurate tracking of the hand and force feedback to the fingers during injection

of Poly(methyl methacrylte) into the bone.

Other simulation systems use mannequins as substitutes for patients to provide orientation and visual clues to the user [9], [10], [11]. Some mannequin based systems incorporate other devices, such as haptic force feedback devices; however, the mannequin is only used as a dummy, with its physical location in space being the only connection to the system. When a mannequin is used solely in a system, the only form of force feedback is provided by the material properties of the mannequin, as no external devices are used to provide forces to the user.

A prominent example of a mannequin based simulator for US guided needle insertion procedures is presented by Magee *et al.* [9]. The group uses a gel based mannequin for their work, and a dummy US probe and a biopsy needle. The mannequin is scanned using a 3D scanner and its surface is manually segmented to obtain an outline in 3D. A patient 3D CT volume is registered to the mannequin CT. The dummy US probe and biopsy needle are tracked using 3D motion sensors, which allow their positions to be known relative to the mannequin/CT volume. The group simulates an US image from the CT volume of the patient. The only form of force feedback provided to the user during needle insertion is the material properties of the mannequin.

Examples of systems that attempt to incorporate mannequins into VR training environments are discussed by Gorman *et al.* [10], Ra *et al.* [11], and Harders *et al.* [12]. Gorman *et al.* present a simple lumbar puncture simulator which uses a PHANToM haptic device with attached needle that runs through the length of a mannequin. The force is calculated using multiple haptic bounding boxes for each tissue type [10]. Ra *et al.* present a system to simulate a spinal biopsy procedure, with one haptic device. The mannequin is used to overcome the shortcomings of a haptic device by physically constraining the needle to move only along a desired path. A patient's CT volume is used as the input to the system, and also the basis for the force model. An "after action" report is generated upon completion of a procedure, with information such as time to target, the trajectory followed, and the error distance from the target [11]. Harders *et al.* outline a system which overlays simulated soft tissue information on a tracked leg mannequin, where a head-mounted display provides visual feedback to the user. A haptic device is used to deform the simulated soft tissue information. System calibration, synchronization and latency are also studied [12].

From the review of mannequin-based training systems, it is clear that most systems do not use a mannequin to its fullest potential. They either use the mannequin as a stand-in, or to physically restrict a needle to a certain insertion direction. The need for combining haptics and a physical mannequin for effective ultrasonography training has been previously shown by us [13] and others [14]. Tahmasebi *et al.* showed that the force feedback provided by the haptic device, while useful was not a sufficient feature to provide the same feeling as scanning a real patient [13]. A common improvement requested was a mannequin to provide the evaluators with spatial awareness of the US scanning plane with respect to the patient's anatomy. Blum *et al.* stated that a mannequin combined with in a virtual
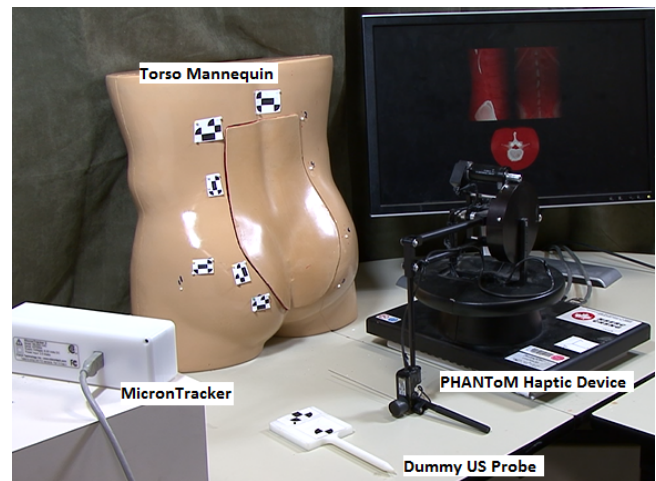

Fig. 1. The system components: Torso mannequin, MicronTracker camera, PHANToM haptic device, dummy US probe and monitor.

reality display enabled the user to explore the use of US and learn how a certain anatomy looks like in US, the effects of occlusion in the images and where to correctly place the probe to see a certain part of the body [14].

Purely VR systems do not use a physical reference in their work space, and only rely on virtual images for visual feedback. Work which aims to combine a mannequin with VR, such as for medical simulation of birth [15], for needle biopsies [16], for liver ablation [17], and for US guided needle biopsies [18] either rely on phantom models for feedback response, or do not consider force feedback.

We present a VR haptic training simulator that incorporates an optically tracked mannequin, a warped CT volume, a simulated US image of the corresponding examination plane and a haptic device. This unique combination has several advantages specifically for US imaging training: i) It provides a physical reference between the US probe held by a sonographer to a mannequin and a simulated US from the virtual patient on the monitor; ii) It enables the dynamic view of the deformations in the anatomy that parallel those observed in real US imaging scenarios due to various probe pressures. The inclusion of finite element modeling of the tissue with real-time US update from a prior CT enables this characteristic; iii) By integrating a haptic device into the VR and mannequin frameworks, the system allows for more flexible force feedback generation via simulation of differing patient bodies; iv) The use of the haptic device for needle insertion enables realistic simulation of a force profile that a clinician would observe during the insertion of a needle through the various tissue layers surrounding the spine, independent of the material properties of the physical mannequin.

The proposed prototype system for spinal insertion simulation has the potential for use as a clinical training tool. The system allows a user to perform a virtual operation on a mannequin which has been registered to patient CT data. The mannequin will provide the user with a physical reference while navigating the virtual patient and the registered CT data set is used to provide an augmented reality overlay on the video feed of the mannequin. By registering the mannequin
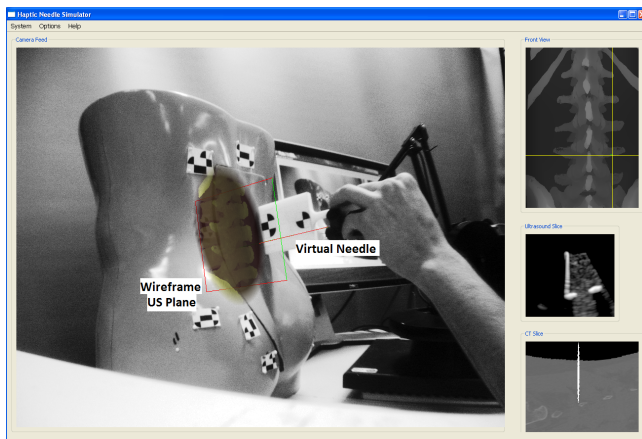
Fig. 2. The developed system in use. The operator is holding an dummy US probe against the mannequin, while observing the corresponding CT re-slice and simulated US image from the probe orientation.

Fig. 3. Needle guide highlighted on the PHANToM stylus. The two images show the needle prior to (left) and after (right) insertion.

to a patient-specific data set and tracking it in 3D space, the proposed system integrates the mannequin into the system. As a result, the proposed system addresses the drawbacks of both types of simulation systems by utilizing the benefits of both to their fullest. This paper will discuss different aspects of the designed system, as well as will present a user impact study on the functionality of a prototype of the proposed system, and its potential as a training tool.

II. System Description

A. System Hardware

Figure 1 provides an overview of the system components and Figure 2 shows the system being operated by a user, holding a dummy US probe and haptic device. The system is composed of a torso mannequin (Sawbones Inc., Vashon, WA) that provides a physical object that is tracked using MicronTracker2 (Claron Technologies, Toronto, ON) optical tracking system and a set of specially designed markers. The mannequin has been registered to a patient-specific CT volume. The MicronTracker2 is the foundation of the augmented reality display, as it provides a video feed and functions that project locations in its camera space onto the image plane. The camera is shown on the left of Figure 1 looking towards the mannequin in the centre. The camera tracks the markers on the mannequin, as well as the dummy US probe, and sends the tracking information back to the PC to compute the augmented reality overlay.

The force feedback necessary to create the feel of a needle insertion is provided through the use of a Geomagic (Wilmington, MA) PHANToM Premium 1.5A haptic device with three degrees of active feedback along the translational axes, and additional three passive DOF along the three rotational axes. The haptic device interacts with a finite element model (FEM), obtained based on the patient CT volume, to generate output forces for the user and deformations for the volume. A PC with a CUDA enabled NVidia graphics card provides the visual feedback to the user via a monitor.

A needle is attached to a guide that is allowed to slide freely along the stylus of the haptic device, as shown in Figure 3.
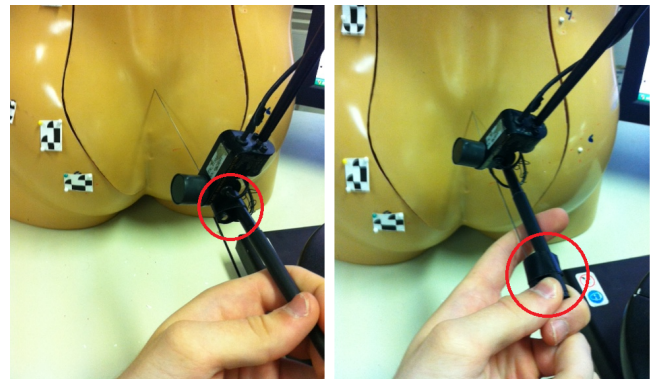
The retractable needle and guide provide a physical reference point for the virtual needle. The attached needle is the same length as the virtual needle, and when it is pressed up against the mannequin, the needle and guide will slide along the stylus of the haptic device, allowing all the force generation to stem from the haptic device and not the physical needle entering the mannequin. This retraction is smooth enough that it produces a negligible force.

B. Software Architecture

The flow of data between functions in the program is visualized in Figure 4. Black arrows show data flow, with the type of data being passed written beside them. The MicronTracker2 camera sends the video feed frames, as well as the positions of the markers, to the visual tracking routine which calculates the position and orientation of the US probe and mannequin. Meanwhile, the PHANToM device sends the position and orientation of the end effector to the FEM routine, which returns the forces calculated by the tissue model. The US simulation routine takes the US probe information as well as the virtual needle tip and mesh deformations calculated from the FEM routine, and simulates an US image from the CT volume data. The video feed frames, as well as the mannequin position is sent from the visual tracking routine to the CT overlay routine. The augmented overlay is computed in the CT overlay routine and sent to the display, along with the simulated US image and CT image.

As shown in Figure 5, the program contains two main loops, one for the graphical display and one for the haptic feedback. The loops have vastly different rate requirements. The graphical loop should run at a rate about 20 Hz, which is the rate required for human vision to not notice lag in visual updates. The haptic loop, on the other hand, must run at a rate much faster (at least 1000 Hz), which will be referred to as the haptic constraint in the future. At rates much lower than this, the system may become unstable for a specific environment dynamic or the force feedback update can become coarsely quantized which can be felt by the user and is not desired [19]. It is therefore necessary to limit calculations in the haptic loop to essential haptic functions and exclude computationally expensive image related functions.
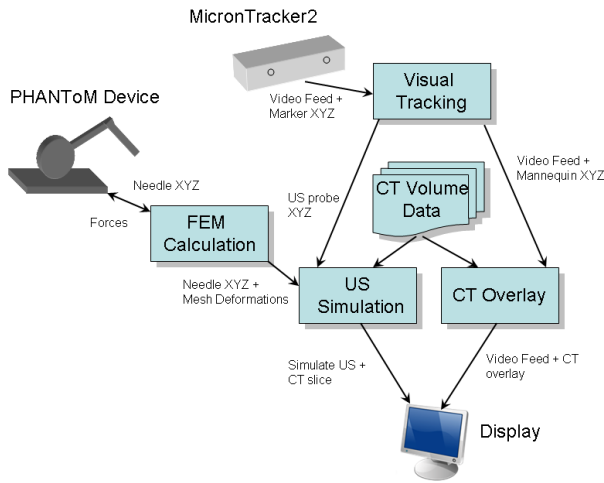
Fig. 4. Data Flow in the program. Boxes represent program functions that input/output data. The type of data is described with each arrow

Fig. 5. System integration for haptic and graphic loops.

The system software has been written in C++ under Microsoft Windows using the Microsoft Visual Studio 2005 compiler. MATLAB was also used for some pre-analysis. Software libraries used included the Visual Toolkit (VTK) [20], the Insight Toolkit (ITK) [21], Sensable OpenHaptics 2.0 architecture for driving input/output to the haptic device, the MicronTracker2 SDK from Claron Technologies to receive information from the MicronTracker camera, and QT to create the graphical user interface (GUI) [22].

C. Virtual Model

There are a variety of models available for modeling tissue deformations, including mass-spring, surface, and finite element based models [23]. A mass-spring model connects many different mass nodes with springs that sometimes cross each other, leading to complicated calculations for the node parameters. A surface model would be useful if deformations were only required to be viewed from outside the volume (looking at the surface), which is not the case for our system, as the deformations we are interested in occur in the interior of the volume. In light of this, the best choice for our system is an FEM.

The second decision that must be made when deciding on a deformation model is the characteristics of the said model; whether a dynamic or static model is desired, and whether it should be linear or non-linear. Since the skin and soft tissue behavior is dominated by elastic responses over small deformations, the small loss in realism caused by a static model is worth the trade off in place of a more computationally expensive dynamic model [24]. Soft tissue is, by nature, non-linear so the most realistic deformations would need a non-linear model. However, over small deformations, the non-linearity can be approximated by linear models [25]. As argued by Cotin *et al.* [24], the integration of force feedback allows the range of tissue deformations to be controlled. As the deformation increases, the force being generated by the FEM will increase accordingly, preventing the deformations from becoming too large. In addition, the reported maximum
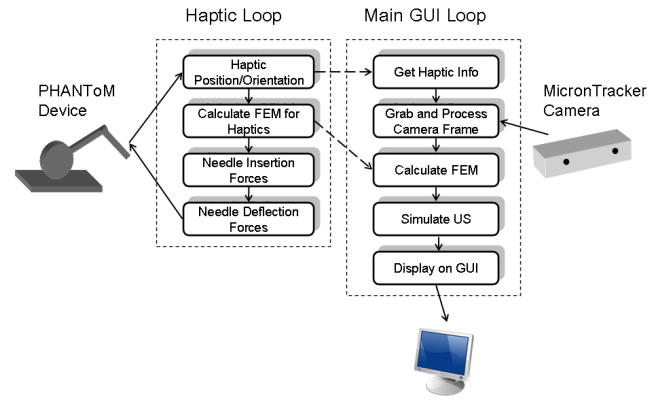
deflection for 25-gauge symmetric spinal needles for large insertion depth, e.g. $60\,,mm$, is below $0.5\,,mm$ [26], which is very small. Therefore, similar to [11], a linear elastic FEM model is considered to represent the deformations.

Surgical needles that are commonly used in spinal anesthesia procedures act fairly rigidly in soft tissue. Since deflections during spinal anesthesia procedures are generally small, and a needle bending model was deemed too computationally expensive [27], the virtual needle is modeled by a rigid, symmetric, 24-gauge needle.

The FEM of the object is defined by a 3D mesh of tetrahedral polygons [28]. The combined elastic effect of each polygon can be presented by the linear elastic FEM equation

$$\vec{f} = \mathbf{K}\vec{u}. \tag{1}$$

where $\vec{f}$ is the global force vector acting on the body at the insertion point, and $\vec{u}$ is the global displacement vector [28]. The force and displacement vectors are of length $3N \times 1$, where N is the number of nodes in the system. For any node i, the elements $3i - 2, 3i - 1$ and $3i$ correspond to x, y, z components of the node, respectively.

The matrix $\mathbf{K}$ is singular, and any force acting on any node can cause infinite number of displacements. To remedy this issue, we apply boundary conditions to a number of the nodes - the minimum number of nodes needing to be fixed is equal to the dimension of the object. In order to create these boundary conditions, the nodes of the mesh corresponding to the side of the CT volume opposite insertion and those corresponding to bone are set as fixed. The simulation method follows that described by DiMaio in [27]. The tetrahedral mesh was generated from a patient CT scan, segmented into different tissues (soft tissue/ligament/bone). The nodes were closer to each other at boarders between tissue types to capture the tissue inhomogenities. The heaviest concentration of nodes was around the area most likely to be punctured by the needle rather than the actual needle path to eliminate the need to re-calculate the FE mesh and its equations every time the needle re-entered the body. To generate the mesh from the nodes, the 3D Delaunay triangulation method was used via MATLAB. The parameters of the model, Youngs modulus and the Poisson's ratio, were selected from values found in the literature ([29], [30], [31]), and can be seen in Table I.
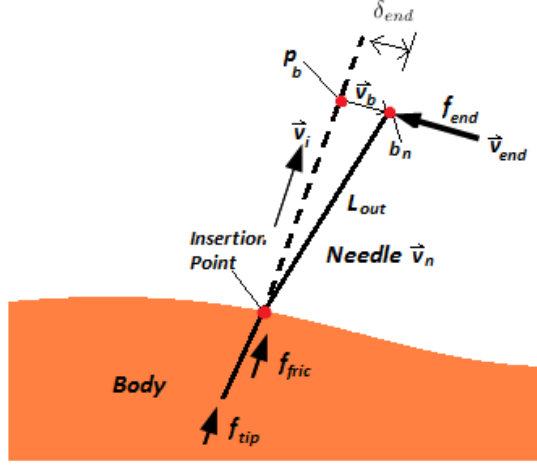
Fig. 6. Forces and displacements for an inserted needle under deflection. Original insertion vector $\vec{v}_i$, current needle vector $\vec{v}_n$, direction of bend $\vec{v}_b$ at the base of the needle, end force due to bending f_{end}, and forces from the tip f_{tip} and friction f_{fric}.

TABLE I
VALUES FOR MODEL PARAMETERS.

Tissue	Youngs Modulus	Poisson ratio
Soft tissue	20 kPa	.3
Ligament	170 kPa	.3

Inhomogeneity was included in the model via layers of tissue with differing properties.

D. Force Generation

Creating an algorithm for deforming the mesh based on the position of the needle tip is another challenge, as the needle will not always travel along a path that always strikes nodes. Methods of mesh deformations discussed by DiMaio *et al.* [27] include a node snapping/closest node method, mesh adaptation, and re-meshing. Adaptation and re-meshing were determined to be too computationally expensive to run in a haptic loop. Therefore, chose the method of closest node forcing.

The forces from the displacement of the closest node are calculated using (1) and sent back to the haptic device. In addition to the penetration force from node displacement, the needle will also experience a friction force during insertion based on the tissue it is penetrating in [32]. The amount of friction depends on how far into the current tissue the needle has traveled [33], [34]. Since the velocity of penetration is low in our application, we only consider the static effect in our friction model

$$f_{fric} = \sum_t d_t \mu_t, \tag{2}$$

where t is the number of tissue types simulated, d is the length of needle inside the tissue, and μ_t is the static (Coulomb) friction force per unit length along the needle for a tissue type [35]. The total force felt at the base of the needle by the user

is

$$f_{base} = f_{tip} + f_{fric}, \tag{3}$$

where f_{tip} is derived from (1). If the base of a needle inserted inside a body is displaced such that the base moves off the insertion vector, the needle will exert a force opposing the motion to pull it back towards the proper vector, as it acts like a bending rod, with fixed point being the point of insertion. This can be modeled by assuming the needle undergoes bending like a thin cylinder, and using a standard beam deflection model to calculate the forces from bending as a function of the displacement of the needle base (δ_{end}) and length of the needle outside the body (L_{out}):

$$f_{end} = \frac{3EI_n\delta_{end}}{L_{out}^3}, \tag{4}$$

where E is the Young's Modulus and I_n is the moment of inertia of the needle for stainless steel. This gives a force function which will give higher forces the greater the deflection of the needle, and also the further the needle is in the body when deflected.

Figure 6 shows an example of the forces on a deflected needle in a body, where the direction vectors $\vec{v}$ are unit vectors. The needle $\vec{v}_n$ is deflected off of the original insertion direction $\vec{v}_i$ by the amount $\vec{v}_b$. The deflection results in the force f_{end} experienced at the base of the needle. The forces from internal friction along the needle, f_{fric}, and tip force, f_{tip}, are also shown in the figure. As a result, the total force experienced by the user at the insertion point is:

$$\vec{f}_{tot} = f_{base}\vec{v}_i + f_{end}\vec{v}_{end}, \tag{5}$$

where $\vec{v}_{end}$ is the direction of the force created from bending, and $f = f_{tot}$ in (1). The position of the insertion point will change due to the deflection of the needle outside the body. The deflection is applied to the insertion point via ftot, deforming the FEM mesh. The displacement at the insertion point is maintained in memory so that when the FEM grid deforms, the correct insertion point is maintained.
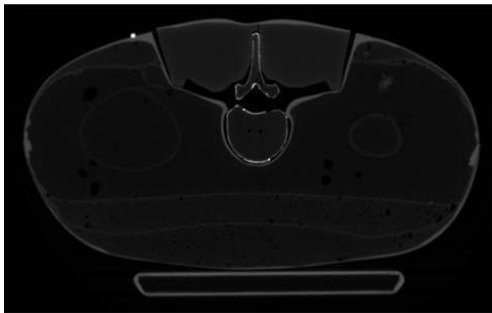
E. Augmented Reality Overlay

In order to provide the users with the maximum information to assist them in guidance, we track a mannequin in 3D with the MicronTracker camera (hereafter referred to as a camera) and overlay a registered patient CT volume onto the video feed of the camera. The mannequin can be used as a replacement for any patient, where the patient CT data is warped to fit its shape. The work in this section is an effort to seamlessly integrate the mannequin into the training system, by tracking it in 3D space and using it as a medium to create an augmented reality visualization by overlaying CT data onto its location in the video feed.

The mannequin interior is foam, with a thin plastic coating to simulate skin. A cutout of the lumbar spine region allows a detailed spine model to be inserted into the mannequin and covered up with an opaque or clear cover. The mannequin, with spine model inserted into cutout, can be seen in Figure 7(a). This mannequin was chosen for two reasons: (1) it is a close representation of a human torso, and (2) the inserted

(a) Picture of the torso mannequin with a spine model in the cutout. CT beads are visible on the right and the MicronTracker markers are shown on the left.

(b) A slice of mannequin CT volume with bead visible at the top left.

Fig. 7.   Mannequin torso with CT visible beads.

Fig. 8.   Final output of CT overlay procedure

spine model would show up on a CT image which would be important for creating the augmented reality overlay function. In preparation for the overlay, the mannequin was scanned with a CT system at our local hospital. Prior to the scan, small round (radius 2 mm) CT visible beads were attached to the surface of the mannequin as well as to the spinous and transverse processes of the internal spine model. The CT beads can be seen on the right side of the mannequin, and markers on the left.

The beads were manually annotated from the CT scan of the mannequin, with the voxel coordinate of each bead recorded. If a bead was on the spine model, the voxel within the bead closest to the bone was chosen, to obtain the location of the bone. For beads on the "skin" of the mannequin, the voxel within the bead furthest from the "skin" was chosen, as tracking markers would be attached to the bead at this location. A sample CT slice of the mannequin showing the beads can be seen in Figure 7(b). In preparation for visual tracking, markers were attached to the side of the mannequin

that would be in view of the camera. L-shaped markers were used, with the center of the middle 3D point being placed directly over the CT visible bead.

A rigid registration scheme with scaling component is used to align a patient CT volume with the mannequin CT. The patient CT is blended with the mannequin so that the skin of the patient is in the same location as the "skin" of the mannequin. The mannequin CT can then be registered with the camera space through markers attached to its surface. When these two registrations are applied to the bounding box of the patient CT volume, it is properly aligned in the camera space with the position and orientation of the mannequin.

Once the two CT volumes have been registered with each other and the camera space, the 3D point in the camera space is passed to the MicronTracker functions to return the (x,y) pixel location on the camera image plane, representing where the ray from the camera viewpoint to the 3D location intersects the image plane. A volume ray casting method is used to create a view of the patient CT in the correct location on the camera image plane to generate the overlay effect [36].

An oval-shaped blending function is utilized to meld the edges of the overlaid image with the background to create the illusion of a cutaway into the anatomy. The oval is centered near the center of the projected 3D bounded box. The falloff function is calculated by finding the length of the vector from the oval origin to the current pixel, and then finding the ratio between this length and the radius of the oval at the angle of the current pixel (r). This gives a percentage of the radius, and for percentages over a certain threshold r_t, the function

$$\alpha = \frac{1-r}{1-r_t} \qquad (6)$$

is used to find the transparency of the pixel. Any value ratio greater than one would be outside the oval and completely transparent, while any value of α lesser than one would only be partially transparent. The final product of the overlaying
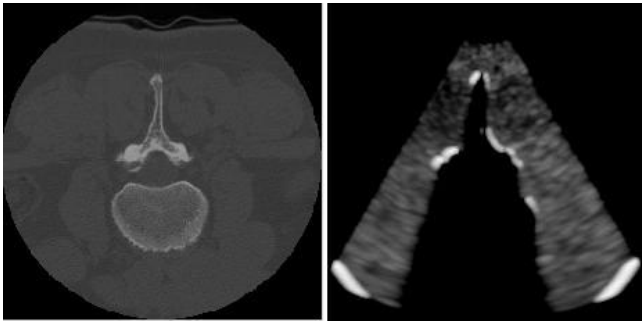
This article has been accepted for publication in a future issue of this journal, but has not been fully edited. Content may change prior to final publication.

7

Fig. 9. *Left*: 2D slice of CT volume. *Right*: Simulated US image.

TABLE II
TEMPORAL COMPARISON OF US SIMULATION FROM CT RE-SLICE FOR A
300×300 PIXEL IMAGE.

Method	Time (ms)
MATLAB	1523
Non-CUDA C++	22
CUDA C++	1.05

procedure can be seen in Figure 8.

F. Ultrasound Simulation

In an US guided procedure, it is necessary to have an US image for the clinician to view. In a simulation system, the US volume of a patient is not always present with other imaging volumes (for example CT or MRI). In these cases, it is necessary to simulate the US image from the data of another imaging modality. The algorithm for the simulation of US from CT is based on the acoustic model presented by Shams *et al.* [37]. The algorithm operates on the assumption that the acoustic impedances of tissue can be calculated from the Hounsfield values in a CT image.

In order to accurately simulate the effects of an US beam, the reflection of the sound waves at boundaries between tissue types must be modeled. At these boundaries there is a change in the acoustic impedance, creating a barrier which only allows a percentage of the sound energy to continue, reflecting the rest back in a scattering pattern. For a homogeneous material with density ρ, the characteristic impedance is defined as:

$$Z = \rho c, \tag{7}$$

where c is the wave speed or in this case, the speed of sound. At a boundary between two materials with acoustic impedance Z_1 and Z_2, the ratio of the sound energy which is reflected is called the coefficient of reflection and found according to:

$$r_\alpha = \frac{Z_2 - Z_1}{Z_2 + Z_1}. \tag{8}$$

To simulate the US image, the US beam is treated as a single ray being cast down each column of the image, losing intensity as it passes through varying mediums in the CT volume. If a curvi-linear probe is used, the polar coordinates are transposed to cartesian coordinates in order to create a recti-linear image which a ray can be cast down. We modified the approach of Shams *et al.* [37] slightly to consider the bone-tissue boundaries in US images, which resulted in brighter
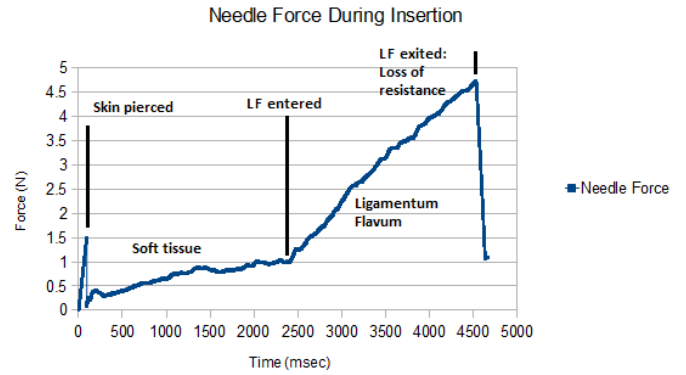

Fig. 10. Force profile during simulated needle insertion versus time for an insertion piercing the ligamentum flavum (LF).

bone edges, and to enforce shadowing artifacts specific to the spine anatomy. An example of a simulated image can be seen in Figure 9. Comparison of this simulation and real US data has been reported elsewhere [38].

The algorithm is implemented in CUDA in order to run on the GPU for increased simulation speed for real time applications. A comparison of the various speeds of the algorithm can be seen in Table II, with implementations in MATLAB, non-CUDA and CUDA C++ compared for a 300×300 pixel image. As can be seen, CUDA implementation improves the simulation speed by over a magnitude, significantly reducing the strain on the graphics loop.

III. RESULTS

To evaluate the features and functionalities of the prototype system, the forces created by the system were recorded during the virtual insertion and compared to the published results, and a user study was conducted to evaluate the potential of the system for use as a training device.

A. System Performance

The system is able to run a 2000 node FEM within the constraints of the haptic loop, and can maintain the update for the graphical loop at up to 20 FPS. In order to objectively analyze the performance of the system, the type of tissues traversed during a virtual needle insertion as well as the forces generated by the model were recorded and shown in the force profile in Figure 10. During the insertion, the force generated by the model at skin puncture was on average 1.5 N, while in soft tissue ranged from 0.5 N to 1.5 N, and when piercing the Ligamentum Flavum (LF) was an average of 4.7N. These values may differ from the ones reported in the literature due to the difference in the gauge of the needle used. For example, Naemura *et al.* [39] has reported peak forces of 5 ± 1 N for piercing the LF of porcine tissue with 18-gauge needles, whereas Brett *et al.* [33] has reported a peak of 9 N with 16-gauge needles. The thicker needle used is responsible for the increased force reported. Although the reported peak values differ due to the needle size, the pattern of the profile in Figure 10 closely follows the one experimental profile reported in [33].

TABLE III
RESPONSES TO MEDIAN SYSTEM FUNCTIONALITY AND THE FEASIBILITY
OF THE SYSTEM AS A TRAINING ENVIRONMENT

No	Question	Gr.1	Gr.2
Functionality			
1	System Purpose clear and understood	6.0	7.0
2	Interaction with system and components is easy and straightforward	6.0	7.0
3	Mannequin is useful for spatial orientation when navigating the body	5.0	7.0
Visual Feedback			
4	AR overlay helpful for initial placement of needle	5.5	5.0
5	Front CT view helpful for initial placement of needle	6.0	7.0
6	AR overlay useful for navigation of patient	5.0	6.0
7	Simulated US images similar to clinical images	5.0	5.5
8	Needle display on screen helpful	7.0	5.5
Haptic Feedback			
9	Can determine skin puncture	7.0	7.0
9b	Skin puncture realistic	6.0	
10	Can determine when needle in soft tissue	7.0	7.0
10b	Soft tissue realistic	5.0	
11	Can determine when loss of resistance is felt	7.0	6.0
11b	Loss of resistance realistic	6.0	
12	Can determine when bone is contacted	7.0	7.0

B. User Study

An important part of system evaluation involves feedback from potential users (subjects). Ten subjects were asked to try the system: four radiology residents with experience with needle insertions (Gr1), and three students and three technicians with experience in viewing US images and with basic understanding of needle insertion procedures (Gr2). The study was approved by the Human Ethics Board of Queen's University and written consent was received from all subjects. The subjects were given a short introduction to the system which included a 1-2 minute overview of its purpose, features and how to interact with it. They were then given 5-10 minutes to explore the system functionality, to familiarize themselves with maneuvering the virtual needle inside the virtual tissue, and to feel the loss of resistance characterizing a successful spinal anesthesia procedure. The subjects were then asked to perform a final trial insertion and fill out a questionnaire on the functionality of the system and its potential as a training system.

The questionnaire answered was composed of three sections: System Functionality, Graphical User Interface (GUI) and Haptic Feedback. The sections were designed to address the important aspects of the system: how functional it was, how the multiple visual aids and graphical interfaces combined to help the user perform the procedure, and if the force feedback felt appropriate. The users were asked to quantify their responses to questions on a scale of 7 with 7 being strongest agreement and 1 being strongest disagreement. The questions asked and the median of the responses can be seen in Table III. We did not perform statistical test to compare the responses of the two groups given the sizes of the groups. However, from Table II, it seems that the two user groups agree on their responses to all questions, except Question 8. For this question, the experienced group was in a stronger agreement that the needle display on screen was useful, pointing at the benefit of this clinical feature of the system.

Functionality: Subjects were able to clearly understand the purpose of the system, and were able to easily interact with all of its components. Both groups of respondents found the mannequin to be useful as a physical reference, for orientating themselves and a good aid for navigating the patient data.

Visual Feedback: The virtual needle display on the video feed, as mentioned above, was found to be useful, specifically the changing of the color depending on the tissue type or if bone was struck. The subjects reported that the simulated US images were somewhat realistic compared to clinical images. The US simulation algorithm enhances bone edges hence the simulated and real US images will not be identical. However, the simulation approach preserves the directionality information of US images of bones. Furthermore, real-time implementation with CUDA enables interactive rendering of images as the US probe moves in space. As a result, the overall experience of the user is positive. Subjects responded favorably to the haptic feedback.

Haptic Feedback: Most could easily tell when skin was punctured, and could feel when the needle struck the bone. When asked to insert the needle between two spinous processes and puncture through the LF, the subjects were able to successfully perform the procedure and feel the increased resistance upon entering the ligament, followed by the "pop through" from the loss of resistance when the needle exits the ligament. Three additional questions were asked from the experienced subjects (Gr1) to determine how they felt the system performed when compared to the real life sensation of piercing skin, traveling through soft tissue and feeling the loss of resistance upon piercing the ligamentum flavum. The experienced subjects reported that the forces felt realistic.

In summary, the subjects responded favorably to the functionality of the system and its potential as a simulation system. Specifically, the positive response from experienced subjects on the haptic feedback was especially motivating.

IV. DISCUSSION

The user study returned positive response on the system potential for use as a training tool. According to the experienced subjects, the combination of virtual force generation and a mannequin created a more realistic simulation along with a physical reference. They also felt that the forces generated by the system were appropriate, specifically the loss of resistance. It is important to note that the positive subject experience with simulated US images is not solely based on comparing the appearance of a single simulated US image with what the user would expect the corresponding real US image to be. Given that the simulation approach is physics based, the directionality information is preserved in US images. This combined with the ability to render images in real-time leads to positive feedback from subjects. In addition to the user study above, three expert clinicians - an ER specialist, an anesthesiologist, and an orthopedic surgeon - were also consulted during the evaluation of the system. All the clinicians were instructors in medical school, and as such, evaluated the system in terms of

its potential for teaching and training purposes, and provided suggestions for improvement.

- Finer segmentation of the CT scan in order to differentiate between different ligaments, and the dura space, allowing users to detect additional failures in needle placement.
- Adding measurement notches to the physical needle so that the user can tell how far into the body the needle is.
- Having trainees use the system without certain aspects of the visual feedback (e.g. without CT overlay), and then perform the procedure again with those features active.
- Allow rotations of the needle within the first few centimeters of the insertion. (For our system, this feature would be without force, as the haptic device only provides feedback for translations.)

One common discussion point that came out of the consultations was to create a "training plan" for trainees using the system. The instructors were in agreement that students should use the graphical aids as a source of "secondary information" and focus on the mannequin and physical needle. Since the patient CT volume is registered to the mannequin, users would be able to palpate the physical mannequin in order to find the gap between spinous processes; the virtual needle is inserted based on this information, and the additional visual feedback is used to determine the accuracy or path of the needle. The physical needle guide attached to the stylus of the haptic device is constructed so that the tip of the physical needle corresponds to the tip of the virtual needle. The guide also allows the needle to slide in along the stylus without puncturing the mannequin when force is applied. This enables the user to align the physical guide with the desired entry position and to feel only the forces created by the tissue model during insertion, while observing the physical needle appear to enter the body while it slides. Interactive simulation and rendering of complex needle-tissue interactions is a challenge, in terms of accuracy and haptic update rate. It has been shown that constraint-based methods could provide more detailed and accurate simulation of needle-tissue interactions [40], [41]. Peterlik *et al.* propose a general method of needle-tissue interaction based on constraints between medical devices and tissue to cover all types of surgical procedures [40]. The method uses compliance mechanisms to couple a low-rate model of the tissue and rigid body, with the high update rate of a haptic device. Chentanez *et al.* use an additional coupling variable to constrain needle and tissue through a rotational matrix transforming the constraints from local needle coordinates to world coordinates [41]. Duriez *et al.* propose a constraint-based method that applies the constraints to the deformable model without requiring re-meshing, followed by evaluation of the method with simulated examples [42].

V. CONCLUSIONS AND FUTURE WORK

This paper presents the basis for a novel augmented reality haptic training system for spinal needle insertion procedures. The proposed system provides additional guidance information to the trainees by integrating a mannequin into a virtual environment, creating an augmented reality overlay, which is projected onto a video feed of the procedure. The system is able to simulate US images from a patient CT volume in real time. A GUI displays the US and CT images, the video feed with augmented reality overlay, and a front view of the CT volume with a crosshairs showing the needle tip.

Two groups of subjects, one with clinical experience with needle insertions and the other with no clinical experience, but knowledge of medical images and needle insertions were recruited for a preliminary user study. The study returned positive reviews on the system functionality and its potential use for training. This study, and consultations with clinicians, provided insight on areas where the system could be improved.

Possible avenues are finer segmentation of the patient CT volume for improved US simulation and enhanced tissue model, a mechanism to retract the needle in the guide, improving the US simulation algorithm to better project the difference between soft tissue and muscle/ligaments, and to obtain *in-vivo* force measurements during actual spinal anesthesia procedures to create a more accurate finite element tissue model.

REFERENCES

[1] K. Kunkler, "The role of medical simulation: An overview," *International Journal of Medical Robotics and Computer Assisted Surgery*, vol. 2, pp. 203–210, 2006.

[2] C. Basdogan, M. Sedef, M. Hardens, and S. Wesarg, "Vr-based simulators for training in minimally invasive surgery," *IEEE Computer Graphics and Applications*, vol. 27, no. 2, pp. 54–66, 2007.

[3] A. Tahmasebi, K. Hashtrudi-Zaad, D. Thompson, and P. Abolmaesumi, "A framework for the design of a novel haptic-based medical training simulator," *IEEE Transactions on Information Technology in Biomedicine*, vol. 12, no. 5, pp. 658 –666, 2008.

[4] T. Coles, D. Melange, and N. John, "The role of haptic in medical training simulators: A survey of the state of the art," *IEEE Transactions on Haptics*, vol. 4, no. 1, p. 5166, 2011.

[5] M. Farber, J. Heller, F. Hummel, C. Gerloff, and H. Handels, "Virtual reality based training of lumbar punctures using a 6 degree of freedom haptic device," *Advances in Medical Engineering*, vol. 114, pp. 236–240, 2007.

[6] F. P. Vidal, N. W. John, A. E. Healey, and D. A. Gould, "Simulation of ultrasound guided needle puncture using patient specific data with 3d textures and volume haptic," *Computer Animation and Virtual Worlds*, vol. 19, no. 2, pp. 111–127, 2008.

[7] W. Chan, D. Ni, W. Pang, J. Qin, Y. Chui, S. Yu, and P. Heng, "Learning ultrasound-guided needle insertion skills through an edutainment game," *Transactions on Edutainment IV*, vol. 6250, pp. 200–214, 2010.

[8] C. Chui, J. S. K. Ong, Z. Lian, Z. Wang, J. Teo, J. Zhang, C. Yan, S. Ong, S. Wang, H. Wong, C. Teo, and S. Teoh, "Haptic in computer-mediated simulation: Training in vertebroplasty surgery," *Simulation and Gaming*, vol. 37, no. 4, pp. 438–451, 2006.

[9] D. Magee, Y. Zhu, R. Ratnalingam, P. Gardner, and D. Kessel, "An augmented reality simulator for ultrasound guided needle placement training," *Medical and Biological Engineering and Computing*, vol. 45, pp. 957–967, 2007.

[10] P. Gorman, T. Krummel, R. Webster, M. Smith, and D. Hutchens, "A prototype haptic lumbar puncture simulator," *Studies in Health Technology and Informatics*, vol. 70, pp. 106–109, 2000.

This article has been accepted for publication in a future issue of this journal, but has not been fully edited. Content may change prior to final publication.

10

[11] J. B. Ra, S. M. Kwon, J. K. Kim, J. Yi, K. H. Kim, H. W. Park, K.-U. Kyung, D.-S. Kwon, H. S. Kang, S. T. Kwon, L. Jiang, J. Zeng, K. Geary, and S. K. Mun, "Spine needle biopsy simulator using visual and force feedback," *Computer Aided Surgery*, vol. 7, no. 6, pp. 353–363, 2002.

[12] M. Harders, G. Bianchi, B. Knoerlein, and G. Szkely, "Calibration, registration, and synchronization for high precision augmented reality haptic," *Trans. on Visual. and Computer Graphics*, vol. 15, no. 1, 2009.

[13] A. Tahmasebi, *A Haptic-Based Ultrasound examination/training system*. Thesis (M.Sc.) Queen's University, 2005.

[14] T. Blum, S. Heining, O. Kutter, and N. Navab, "Advanced training methods using an augmented reality ultrasound simulator," in *Proc. of IEEE Int. Symp. on Mixed and Augmented Reality*, 2009, pp. 177–178.

[15] T. Sielhorst, T. Obst, R. Burgkart, R. Riener, and N. Navab, "An augmented reality delivery simulator for medical training," *International Workshop on Augmented Environments for Medical Imaging-MICCAI Satellite Workshop*, 2004.

[16] M. Rosenthal, A. State, J. Lee, G. Hirota, J. Ackerman, K. Keller, E. Pisano, M. Jiroutek, K. Muller, and H. Fuchs, "Augmented reality guidance for needle biopsies: An initial randomized, controlled trial in phantoms," *Medical Image Analysis*, vol. 6, no. 3, pp. 313–320, 2002.

[17] S. Nicolau, X. Pennec, L. Soler, X. Buy, A. Gang, N. Ayache, and J. Marescaux, "An augmented reality system for liver thermal ablation: design and evaluation on clinical cases," *Medical Image Analysis*, vol. 13, no. 3, pp. 494–506, 2009.

[18] A. State, M. Livingston, W. Garrett, G. Hirota, M. Whitton, E. Pisano, and H. Fuchs, "Technologies for augmented reality systems: Realizing ultrasound-guided needle biopsies," in *Proceedings of the conference on Computer Graphics and Interactive Techniques*, 1996, pp. 439–446.

[19] J. Colgate and J. Brown, "Factors affecting the z-width of a haptic display," in *Proceedings of the IEEE International Conference on Robotics and Automation*, pp. 3205–3210.

[20] W. Schroeder, K. Martin, and W. Lorensen, *The visualization toolkit: an object-oriented approach to 3D graphics*. Prentice-Hall, 1998.

[21] L. Ibanez, W. Schroeder, L. Ng, and J. Cates, *The ITK software guide*, 2nd ed. Kitware, Inc., 2005.

[22] N. Systems, *Using QT*, 2009.

[23] N. Abolhassani, R. Patel, and M. Moallem, "Needle insertion into soft tissue: A survey," *Medical Engineering and Physics*, vol. 29, no. 4, pp. 413 – 431, 2007.

[24] S. Cotin, H. Delingette, and N. Ayache, "A hybrid elastic model for real-time cutting, deformations, and force feedback for surgery training and simulation," *The Visual Computer*, vol. 16, pp. 437–452, 2000.

[25] Y. C. Fung, *Mechanical Properties of Living Tissues*. Springer, 1993.

[26] B. Sitzman and D. Uncles, "The effects of needle type gauge and tip bend on spinal needle deflection," *Anesthesia and Analgesia*, vol. 82, no. 2, pp. 297–301, 1996.

[27] S. DiMaio and S. Salcudean, "Interactive simulation of needle insertion models," *IEEE Transactions on Biomedical Engineering*, vol. 52, no. 7, pp. 1167 –1179, July 2005.

[28] M. Bro-Nielsen, "Finite element modeling in surgery simulation," *Proceedings of the IEEE*, vol. 86, no. 3, pp. 490 –503, 1998.

[29] E. J. Chen, J. Novakofski, W. K. Jenkins, and W. D. O'Brien Jr., "Young's modulus measurements of soft tissues with application to elasticity imaging," *IEEE Transactions on Ultrasonics, Ferroelectrics and Frequency Control*, vol. 43, no. 1, pp. 191 –194, 1996.

[30] A. Nachemson and J. Evans, "Some mechanical properties of the third human lumbar interlaminar ligament (ligamentum flavum)," *Journal of Biomechanics*, vol. 1, no. 3, pp. 211 – 220, 1968.

[31] R. Waters and J. Morris, "An in vitro study of normal and scoliotic interspinous ligaments," *Journal of Biomechanics*, vol. 6, no. 4, pp. 343–348, 1973.

[32] S. DiMaio and S. Salcudean, "Needle insertion modeling and simulation," *IEEE Transactions on Robotics and Automation*, vol. 19, no. 5, pp. 864 – 875, 2003.

[33] P. Brett, T. Parker, A. Harrison, T. Thomas, and A. Carr, "Simulation of resistance forces acting on surgical needles," *Proceedings of the Institute of Mechanical Engineers*, vol. 211, pp. 225–347, 1997.

[34] A. Okamura, C. Simone, and M. O'Leary, "Force modeling for needle insertion into soft tissue," *IEEE Transactions on Biomedical Engineering*, pp. 1707–1716, Oct. 2004.

[35] A. Haddadi and K. Hashtrudi-Zaad, "Development of a dynamic model for bevel-tip flexible needle insertion into soft tissues," in *Proceedings of the International IEEE Engineering in Medicine and Biology Society Coneference*, 2011, pp. 7478–7482.

[36] A. Watt and M. Watt, *Advanced Animation and Rendering Techniques:Theory and Practice*. Addison-Wesley, 1992.

[37] R. Shams, R. Hartley, and N. Navab, "Real-time simulation of medical ultrasound from ct images," *Medical Image Computing and Computer-Assisted Intervention*, vol. 5242, pp. 734–741, 2008.

[38] S. Gill, P. Abolmaesumi, G. Fichtinger, J. Boisvert, D. Pichora, D. Borshneck, and P. Mousavi, "Biomechanically constrained groupwise ultrasound to ct registration of the lumbar spine," *Medical Image Analysis*, vol. 5761, pp. 803–810, 2010.

[39] K. Naemura and H. Saito, "Needle insertion test by porcine ligamentum flavum," in *Proceedings of the World Congress on Medical Physics and Biomedical Engineering*. Springer, 2009, pp. 28–31.

[40] N. Chentanez, R. Alterovitz, D. Ritchie, L. Cho, K. Hauser, K. Goldberg, J. Sewchuk, and J. O'Brien, "Interactive simulation of surgical needle-insertion and steering," *ACM Trans. Graphics*, vol. 88, pp. 1–10, 2009.

[41] I. Peterlik, M. Noucier, C. Duriez, S. Cotin, and A. Kheddar, "Constraint-based haptic rendering of multirate compliant mechanisms," *IEEE Transactions on Haptics*, vol. 4, no. 3, pp. 175–187, 2011.

[42] C. Duriez, C. Guebert, M. Marchal, S. Cotin, and L. Grisoni, "Interative simulation of flexible needle insertions on constraint models," in *Proc. of Medical Image Computing and Computer-Assisted Intervention*, 2009.

Colin Sutherland received the B.Sc. degree in Mathematics and Engineering and the M.A.Sc degree in Electrical Engineering from Queen's University, Canada in 2009 and 2011, respectively. He is currently a Systems Engineer with Grantek Systems Integration in Burlington, ON.

Keyvan Hashtrudi-Zaad received his Ph.D. degree in Electrical and Computer Engineering from the University of British Columbia, Canada, in 2000. He is currently the Director of BioRobotics Laboratory and an Associate Professor in the Department of Electrical and Computer Engineering of Queens University. His research interests are in telerobotics, haptics, modeling and controls, and their applications in biomedicine. He is an Associate Editor of IEEE Transactions on Haptics.

Rick Sellens has been on the faculty of Mechanical and Materials Engineering at Queen's since 1989. His research has included the fluid mechanics of sprays, optical instrumentation and imaging systems, and most recently biomechanical and orthopaedic instrumentation and prediction of kinematics.

Purang Abolmaesumi received his Ph.D. degree (2002) from the University of British Columbia (UBC), Canada in Electrical Engineering. From 2002 to 2009, he was a faculty member at Queens University. He then joined the Department of Electrical and Computer Engineering at UBC , where he is a Canada Research Chair and an Associate Professor. Dr. Abolmaesumi's research interests are in ultrasound image processing and image-guided interventions. He is an Associate Editor of IEEE Transactions on Biomedical Engineering.

Parvin Mousavi received her M.Sc. and D.I.C. degrees from the Imperial College, UK, and her Ph.D. from the University of British Columbia, Canada. She is an Associate Professor at the School of Computing, Queen's University, Canada with research focus on computer-assisted interventions and diagnosis. She is the reciepient of the Ontario Early Researcher Award and the Outstanding Young Computer Science Researcher Prize from the Canadian Association of Computer Science.